NBSIR 83-1686

PRELIMINARY EXAMINATION OF 20 GHz G/T MEASUREMENTS OF EARTH TERMINALS

D.F. Wait
W.C. Daywitt

National Bureau of Standards
U.S. Department of Commerce
Boulder, Colorado 80303

March 1983

NBSIR 83-1686

PRELIMINARY EXAMINATION OF 20 GHz G/T MEASUREMENTS OF EARTH TERMINALS

D.F. Wait
W.C. Daywitt

Electromagnetic Fields Division
National Engineering Laboratory
National Bureau of Standards
U.S. Department of Commerce
Boulder, Colorado 80303

March 1983

Prepared for:
U.S. Army Communications Electronics Command
Fort Monmouth, New Jersey

U.S. DEPARTMENT OF COMMERCE, Malcolm Baldrige, Secretary

NATIONAL BUREAU OF STANDARDS, Ernest Ambler, Director

CONTENTS

Preliminary Examination of 20 GHz G/T Measurements of Earth Terminals

David F. Wait and William C. Daywitt

National Bureau of Standards
Boulder, Colorado 80303

Three basic measurement techniques and the associated measuring systems are examined to determine which are most likely to meet the needs for measuring the figure of merit (G/T) of future 20 GHz satellite systems: use of the Sun as a known source, use of the Sun as an intercomparison source with a calibrated reference terminal, and the use of a satellite signal as an intercomparison source. It is shown that the method of using the Sun as a known source is not very accurate (about 1.5 dB uncertainty), but that using the Sun as a transfer source is useful (0.3 dB to 0.5 dB, depending on measuring system) for Earth terminals with antenna diameter less than 1.8 m (6 ft). For Earth terminals with antenna diameters greater than 1.8 m (6 ft), the Sun cannot be used as a transfer source for technical reasons, but a satellite signal can be used as a transfer source.

Key words: automated noise measurements; diffusive attenuation; figure of merit (G/T); lunar star-shape factor; millimeter wave; Moon flux; noise equivalent flux; noise measurement; satellite communications; six-port; Sun flux.

1. OBJECTIVE

The objectives of this initial effort were to (1) determine which measurement techniques and systems are most likely to meet the needs for future 20 GHz satellite systems, (2) estimate the accuracy and repeatability associated with these techniques, and (3) produce estimates of the cost and time required to develop, evaluate, and implement the required measurement systems and techniques.

2. BACKGROUND

One of the more popular specifications of antenna system noise is the figure of merit, usually denoted as G/T [1-11]. Figure of merit is defined to be the ratio of the antenna receive gain to the system noise temperature (referred to as the antenna output port). Figure of merit has the advantage of being a relatively easy noise parameter to measure (for most antenna systems). It can be shown that the figure of merit does not depend on which internal reference plane is selected as being the output port of the antenna. Thus, one can say that the figure of merit is the ratio of the system gain to the system noise temperature [7].

The figure of merit (G/T) has some shortcomings for the precise characterization of the noise of an Earth terminal because it neither characterizes

the hardware, nor the hardware plus atmosphere. This is because the atmospheric effects are excluded from the antenna gain (G) part of G/T, but are included in the system temperature part (T). So, in addition to using the measurement data to calculate G/T, one should also calculate the noise equivalent flux (NEF). NEF characterizes the hardware only. It is a measure of the noise performance of the Earth terminal analogous to effective input noise temperature for an amplifier [12]. NEF is the magnitude of an ideal white, random noise flux density [W m^{-2} Hz^{-1}] incident normal to the aperture of a noiseless equivalent Earth terminal operating in a lossless atmosphere such that the output noise power equals the output noise power of the actual Earth terminal.

2.1 Available Techniques

The noise that originates within or enters into a microwave communication antenna system is a basic characteristic of the system. There are four methods used to make system noise measurements in antenna systems. The first method is to make precision noise and gain (or loss) measurements for the various components of the system and combine these results in an appropriate manner to obtain an overall system noise. In evaluating the characteristics of the individual components, three keys to the overall accuracy for the system noise measurement are the accuracy of measuring (a) the antenna gain [13-17] (NBS calibration services use near field [18-20] or extrapolation [21] techniques), (b) the antenna noise [22], and (c) the amplifier noise [23-25].

A second method is useful for large antenna systems that can "see" a radio star such as Cassiopeia A, the Sun, or the Moon. The known noise from the radio star can be used as a reference to measure the system noise [3,17,22,27]. A third method is to use the signal of known intensity from a satellite. This satellite signal can be used in a way not too different than that of a radio star [4]. Lastly, a modified gain comparison technique can be used where one antenna is basically used to calibrate the strength of some radio source in order to then calibrate a second antenna.

2.2 The Existing NBS Precision G/T Measurement Program

The National Bureau of Standards (NBS) has been making precision noise measurements of antenna systems using radio sources for about ten years [1,12]. Initially, the radio star Cassiopeia A (Cas A) was used [2,28-29], but recently we have begun using the Moon [30] and have made rather extensive preliminary investigations of using the Sun. The uncertainty of the noise measurements in X-band is typically between five and ten percent for systems with antenna gains between 51 dB and 65 db. In general, this method is applicable when (a) the antenna system can "see" the radio source with a signal-to-noise ratio of better than 0.2 (0.8 dB), (b) the half-power beamwidth (HPBW) of the antenna radiation pattern is greater than the diameter of the radio source being used, and (c) the antenna can be pointed at the radio source to a resolution of better than 10% of the HPBW.

2.2.1 The Radio Star Measurement Method

To determine G/T using radio sources, one measures the ratio (Y) of the output noise power when the Earth terminal antenna is pointed at a radio

"star" to the output noise power when the antenna is pointed to the nearby cold sky. The noise power out of the antenna system when the antenna is pointed to a radio source is the power at the output of the antenna times the gain (g) from the antenna output to the system output. Thus,

$$\text{Power out (on source)} = g\ k\ (\Delta T + T)\ B,$$

where ΔT is the temperature rise due to the radio source at the antenna output port, and T is the system temperature expressed relative to the antenna output port, and

$$\text{Power out (on sky)} = g\ k\ T\ B.$$

The ratio of these two measurable powers is,

$$Y = (\Delta T + T)/T. \tag{1}$$

The temperature of the cold sky is included in T. The temperature rise ΔT caused by the star depends on its flux density, $S(W\ m^{-2}\ Hz^{-1})$, and on the effective area of the antenna A_e (m^2),

$$\Delta T = (1/2)\kappa\ SA_e/k, \tag{2}$$

where κ is the correction factor near unity that accounts for the atmospheric loss, star shape, antenna pointing, polarization effects, and instrumentation effects; and k is Boltzmann's constant, $(k = 1.38045 \times 10^{-23} J/K)$. The factor 1/2 in (2) accounts for the fact that only one polarization of radiation can be received from a star at any one time. To introduce the receive gain G, one uses the following relationship,

$$A_e = c^2\ G/(4\ \pi\ f^2) \tag{3}$$

where c is the velocity of light $(2.99793 \times 10^8$ m/s), f is the frequency; so

$$G/T = (Y-1)\ \ (8\ \pi\ k\ f^2)/(\kappa\ c^2\ S)\ , \tag{4}$$

or expressed in decibels above one inverse kelvin,

$$G/T\ (dB/K) = 10\ \log\ (G/T). \tag{5}$$

By replacing T by $(NEF\ A_e)/(2k) + T_{sky}\ (A_e/A_{eo})$, where T_{sky} is the noise power originating from the atmospheric losses plus the three kelvin cosmic background temperature, and A_{eo} is the antenna effective area at the antenna aperture (i.e., no resistive antenna losses included), then the Y-factor (1) becomes

$$Y = (\kappa\ S + 2\ k\ T_{sky}/A_{eo} + NEF)/(2\ k\ T_{sky}/A_{eo} + NEF). \quad (6)$$

Boltzmann's constant, k, and the antenna effective area, A_{eo}, are used to convert T_{sky} to a power density expressed in watts/meter^2. Rearranging (6) we can obtain

$$NEF = \kappa\ S/(Y-1) - 2\ k\ T_{sky}/A_{eo}. \quad (7)$$

2.2.2 NBS G/T Measurement System

To measure the system noise in a large antenna system, the NBS developed the Earth Terminal Measuring System (ETMS) [12,31-34]. The ETMS is a computer-aided measuring system that calculates the pointing angle for the antenna. It also contains a very accurate noise power ratio measuring system (0.1% uncertainty) to measure the noise from the antenna system as the "radio star" drifts through the antenna pattern in five equally spaced declination cuts. The resulting antenna-star response is fit to a three dimensional Gaussian curve.

2.2.2.1 Instrumentation

The ETMS is an automated measurement system. A simplified block diagram of the ETMS is shown in figure 1.

The ETMS contains nine subsystems: (1) A calculator which provides computation capability, a means of controlling each of the remaining subsystems under automatic sequence control, a means of storing the measurement results on magnetic tape in order to rework the data at a later time, and a keyboard to control the measurement procedures or to enter program modifications. (2) An external cassette which allows redundant recording of measurement data. (3) An NBS type IV self-balancing power meter used to measure noise power. (4) A programmable voltmeter. (5) A multiplexer which connects the digital voltmeter to various measurement points of interest. (6) A digital clock to provide required time information to determine current star coordinates. (7) Dual solid state noise source to provide a stable reference signal needed to eliminate the effects of gain fluctuations in the Earth terminal. (8) An rf control unit which provides signal conditioning, system test signals, and the precision circuits which allow the calculator to control the various measuring instruments. (9) A coaxial switch under computer control which allows the input of the rf control unit to be connected to any of three down converters of the Earth terminal.

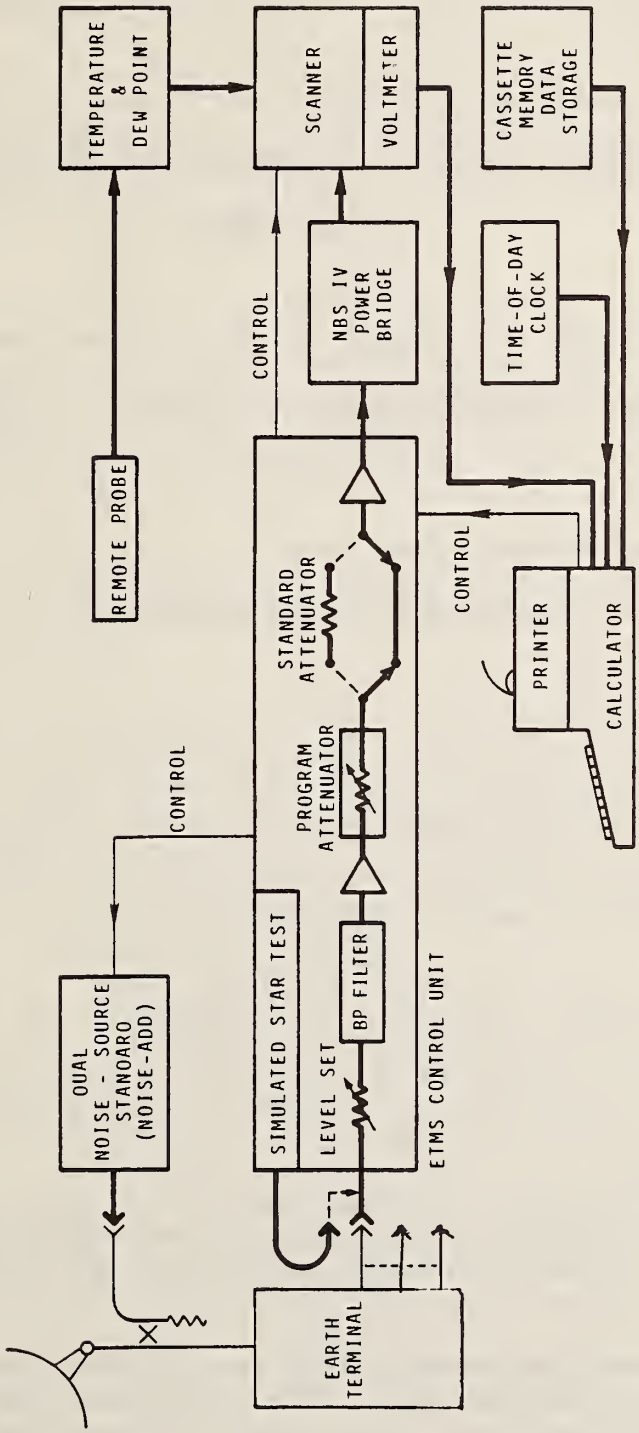

Figure 1. Earth Terminal Measuring System block diagram.

2.2.2.2 Measurement Procedure

The measurement procedure of the ETMS is designed to measure G/T, NEF, and to estimate the antenna gain. The measurement procedure contains the nine steps listed in Table 1.

TABLE 1. Steps in the Measurement Procedure.

STEP	PURPOSE
(PRELIMINARIES)	
1	Prepare daily data tapes, one for each measurement day
2	Validate hardware and tapes before shipping to antenna site
(DATA ACQUISITION)	
3	Validate hardware after arrival
4	Determine antenna offsets, sky profile
5	Collect data
(DATA ANALYSIS)	
6	Split multiple frequency data files into single frequency data files
7	Replace isolated bad data points
8	Obtain best fit parameters for data sets
9	Calculate G/T, etc., and plot results

Many of these steps are self-explanatory. In step 4, sky profile refers to a measurement of the sky temperature versus antenna elevation along the star trajectory. The sky profile is used as an additional check on the atmospheric loss.

In step 5, the measurement data are collected for G/T and NEF. A measurement set contains six cuts. For a cut, the antenna is pointed to a computed coordinate position; then a string of power measurements (typically 30) relative to a reference "noise add" signal are taken 6 seconds apart as Cas A or the Moon drift through. One cut is taken on the cold sky about 2 degrees away (in declination) from Cas A or the Moon. The remaining cuts are spaced equidistant throughout the main beam of the antenna pattern. For the string of power measurements, the ETMS is sequentially connected to the out-

puts of one, two, or three different down converters so that the information for one, two, or three frequencies are collected within one measurement set. The data are stored and G/T, NEF, HPBW's, and the updated antenna point offsets are calculated and printed out.

After all the data have been taken, the remaining steps may be done after leaving the measurement site. Any isolated bad data points are removed from the data sets. Then each data set is least squares fitted to a three-dimensional Gaussian curve and the values for G/T, NEF, and HPBW are calculated using the precision fit results. The last step is to plot and tabulate all of the results as a function of antenna elevation.

2.2.3 Accuracy Considerations

For the measurement of system noise, the noise from a radio star is used as a reference signal. To obtain an accurate measurement, careful attention is given to atmospheric effects, antenna pointing, accurate noise power measurements, adequate characterization of the radio source, and careful calculation of the "star shape" correction factor.

Typically, the uncertainty in the accuracy of the flux of the radio "star" dominates the total measurement uncertainty unless the antenna system is just barely able to observe the radio "star" (i.e., signal-to-noise ratio of less than about 0.1) [2].

The atmospheric effects fall roughly into three categories: absorptive attenuation, diffusive attenuation, and refractive attenuation. The absorptive attenuation is small enough that simple approximate algorithms for the losses, based only on local temperature, humidity, and the site elevation can be used [35]. However, the diffusive attenuation is rather troublesome because of the scarcity of experimental and theoretical information to predict its magnitude and its uncertainty [36-37]. These atmospheric effects are important sources of measurement uncertainty.

Most recently, the NBS measurements have been improved by including a more accurate procedure for measuring the increase of noise caused by the radio "star," and by developing an algorithm which enables the use of the Moon as a precise noise source for broad beam antennas. The ETMS measures the noise power ratio from the antenna system as the "radio star" drifts though the antenna pattern in five equally spaced declination cuts. The resulting antenna-star response is fitted to a three-dimensional Gaussian curve. The accuracy of the antenna system noise ratio measurement is directly related to the accuracy with which the amplitude of this three-dimensional Gaussian curve can be fit, and to how adequately the Gaussian curve represents the true star-antenna convolution output. The fitting procedure is complicated by the time varying radiation coming from the sky. This variation is caused by changes in the atmospheric conditions along the path of the antenna beam.

There are three major sources of error associated with the ETMS measuring system. First is the accuracy with which the noise power ratio from the Earth terminal is measured; second is the accuracy with which the measurement system can respond to the change in power as the radio star drifts through the antenna pattern; and last is the degree of immunity of the measurement to the gain instability of the Earth terminal. In the ETMS, the power is measured

with an NBS type IV power meter [38] which measures the ratio of stable noise powers to an accuracy of better than 0.1%. The ETMS responds to changes in power level as the star drifts through to an accuracy of better than 0.2%. The effects of gain variations in the Earth terminal under test are suppressed by utilizing a noise adding technique [39]. The stability of the noise source over the 30 minutes required to make a complete measurement set is better than 0.6% [40].

2.3 NBS Automated Noise Measurements

Some of the measurements discussed in this report require a calibrated noise source. At the present time, no noise calibration service exists at 20 GHz. If it proves necessary to establish a 20 GHz service, it would incorporate the automated radiometer currently under construction, and would be implemented in a way similar to the 94 GHz section of radiometer which is now entering the final phases of construction. To understand this better, a short overview of the NBS automated noise measurements, and particularly the 94 GHz section of the automated noise radiometer is presented.

The National Bureau of Standards uses two different automated noise radiometers which are used for noise calibration services. One has been used to calibrate noise sources in WR15 waveguide (56 GHz to 64 GHz) since 1972 [41]. The other, still under construction, is scheduled in the next five years to measure coaxial noise sources in the frequency range between 30 MHz and 12 GHz, and waveguide noise sources in WR284 (2.6 GHz to 3.95 GHz), WR90 (8.2 GHz to 12.4 GHz), and WR10 (94 GHz to 95 GHz). Only the 30 MHz and 60 MHz segments of the coaxial radiometer are currently being used in calibration services [42].

Both of these radiometers, like the ETMS, are systems developed around the NBS type IV self-balancing rf power meter [38]. The radiometers incorporating this power meter measure the ratio of stable noise powers to an uncertainty of less than ±0.1%. The proof of this measurement accuracy is accomplished in stages. First, an initial verification of measurement accuracy; then, a validation that the measurement accuracy has not changed. The measurement accuracy depends on the accuracy of the power meter and on the linearity of the amplifiers in the radiometer. Each of these sources of uncertainty are studied separately, and then the overall uncertainty is examined.

For example, in the WR15 radiometer, the initial verification of measurement accuracy was examined using a matched precision rotary vane WR15 attenuator at the front end of the radiometer. This attenuator was constructed and adjusted so that it followed very closely the theoretical dependence on the attenuator vane angle [43]. By comparing the measured changes at the output of the radiometer with the known changes of power (and correcting for the noise originating within the radiometer), as shown in figure 2, an upper bound for the linearity of the radiometer was determined. That is, the physical principles of changing the power into the radiometer (rotary vane attenuator), and that of measuring the power out of the radiometer (type IV power meter) are independent. Thus, within the error that one tracks the other, they both must be known. Accidental error subtractions can be eliminated by changing the initial source power level.

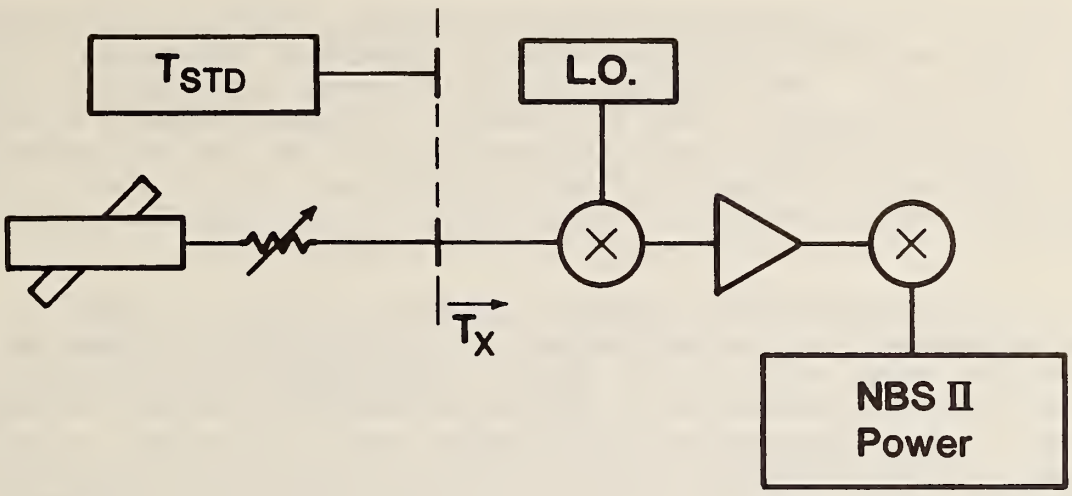

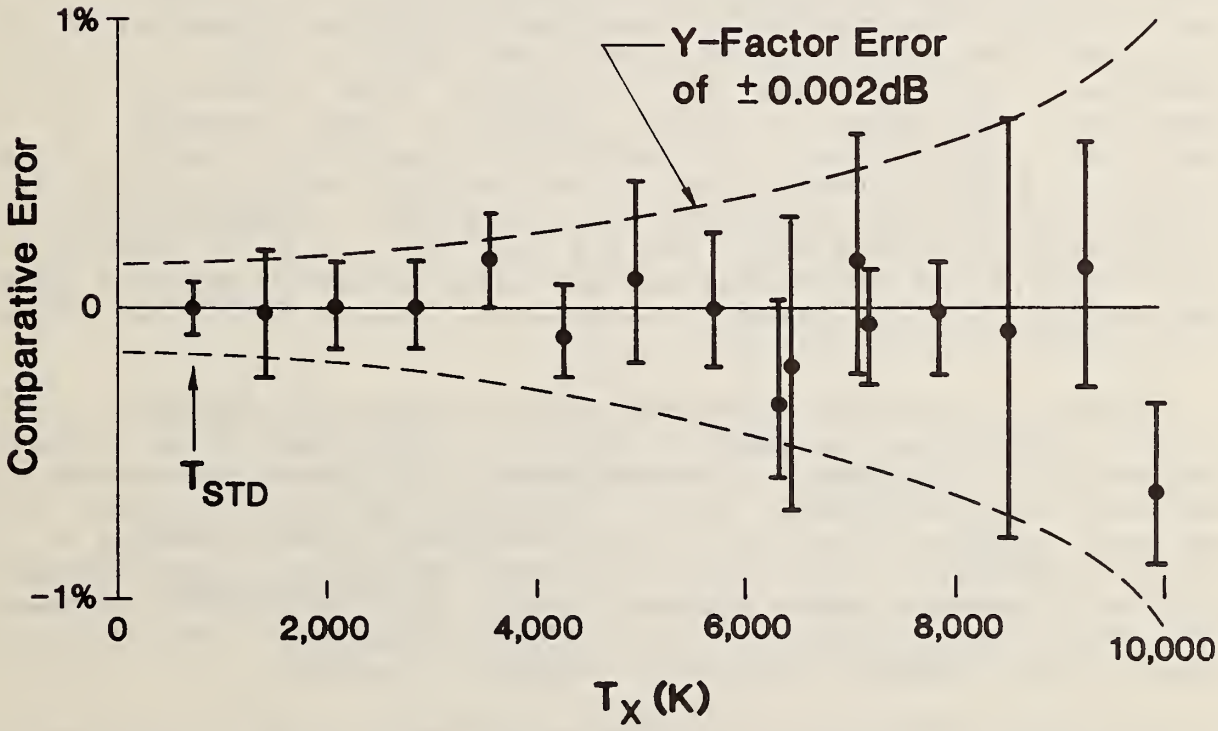

Figure 2. Error in measuring known WR15 noise source.

The goal of the NBS is to transfer the bulk of the noise measurement and calibration services onto automated noise comparison radiometers within the next five years. These systems provide improved measurement control and require less maintenance. They also provide continuous frequency coverage and enable the NBS to offer noise measurement services for the much needed satellite communication frequencies that heretofore were not available. Further, calibration time is reduced; in some cases, 8 to 10 frequencies can be calibrated in the time formerly required for one frequency.

A block diagram of the automated radiometer is shown in figure 3. A more detailed schematic of the radiometer, as it exists now, is shown in figure 4. On the right hand side of figure 4 are shown the 30 MHz and 60 MHz sections that are currently being used in calibrations. On the left hand side is the 2 - 4 GHz section of the radiometer, and in the center is the 94 GHz section of the radiometer. If a 20 GHz noise calibration service is implemented, then a 20 GHz section similar to the 94 GHz section would be added.

The 30 MHz and 60 MHz noise calibrations have a typical calibration uncertainty of about 1%, which is comparable to the uncertainty of the retired manual calibration system [44]. The measurement procedure for this service uses three solid-state noise check standards (which are switched into the measurement sequence automatically), and one cryogenic check standard. Two of the solid state noise sources have permanently connected attenuators so that the output of the solid state noise sources are 11,050 K, 5,755 K, and 3,055 K respectively, and the output of the cryogenic check standard is 77.1 K. Significant with regard to their function as check standards is the measurement repeatability. The measurement repeatability depends on the resolution of the radiometer, and on the long term stability of the check standard sources. Over six months, the system/source repeatability has been 11,050 K ± 20 K, 5,755 ± 10 K, 3055 K ± 10 K, and 77.1 ± 1 K. Because the check standards have outputs that span the normal calibration amplitude range, the linearity of the radiometer is automatically assured during the calibration cycle.

Other than at 30 MHz and 60 MHz sections, each front end begins with a six-port reflectometer as shown in figure 5. This allows for an automated compensation of the mismatch difference between the standard noise source, and the source being calibrated. Another feature is the use of cryogenic noise standards. Although this results in poorer relative radiometer resolution, it has the advantages of being easier to maintain and to use so that it becomes practical to use the primary standard directly in the calibration procedure. This also allows calibrations at any arbitrary frequency in the calibration range, rather than being restricted to preferred frequencies.

An important feature of the automated radiometer is the relative ease in extending calibrations into new frequency bands. Heretofore, frequency extensions were major undertakings. This situation has changed because of several different developments. First, many of the validation procedures are automated, and the computer programs and the IF section of the radiometer are common to all of the different frequency bands. Thus, the effort to validate the system at a new frequency is minimal. Secondly, when the coaxial standard

94 GHZ RADIOMETER

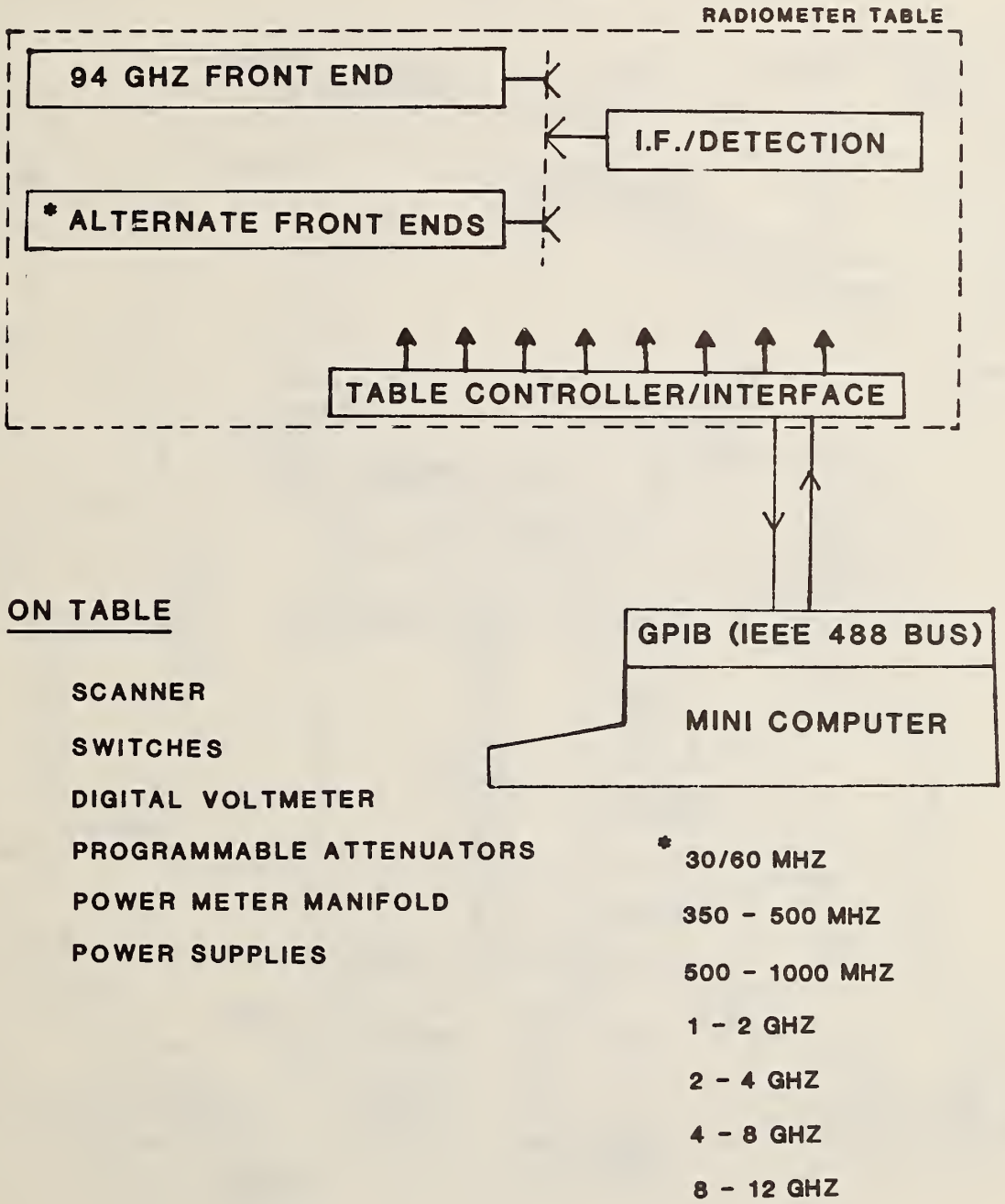

Figure 3. Block diagram of the automated noise radiometer.

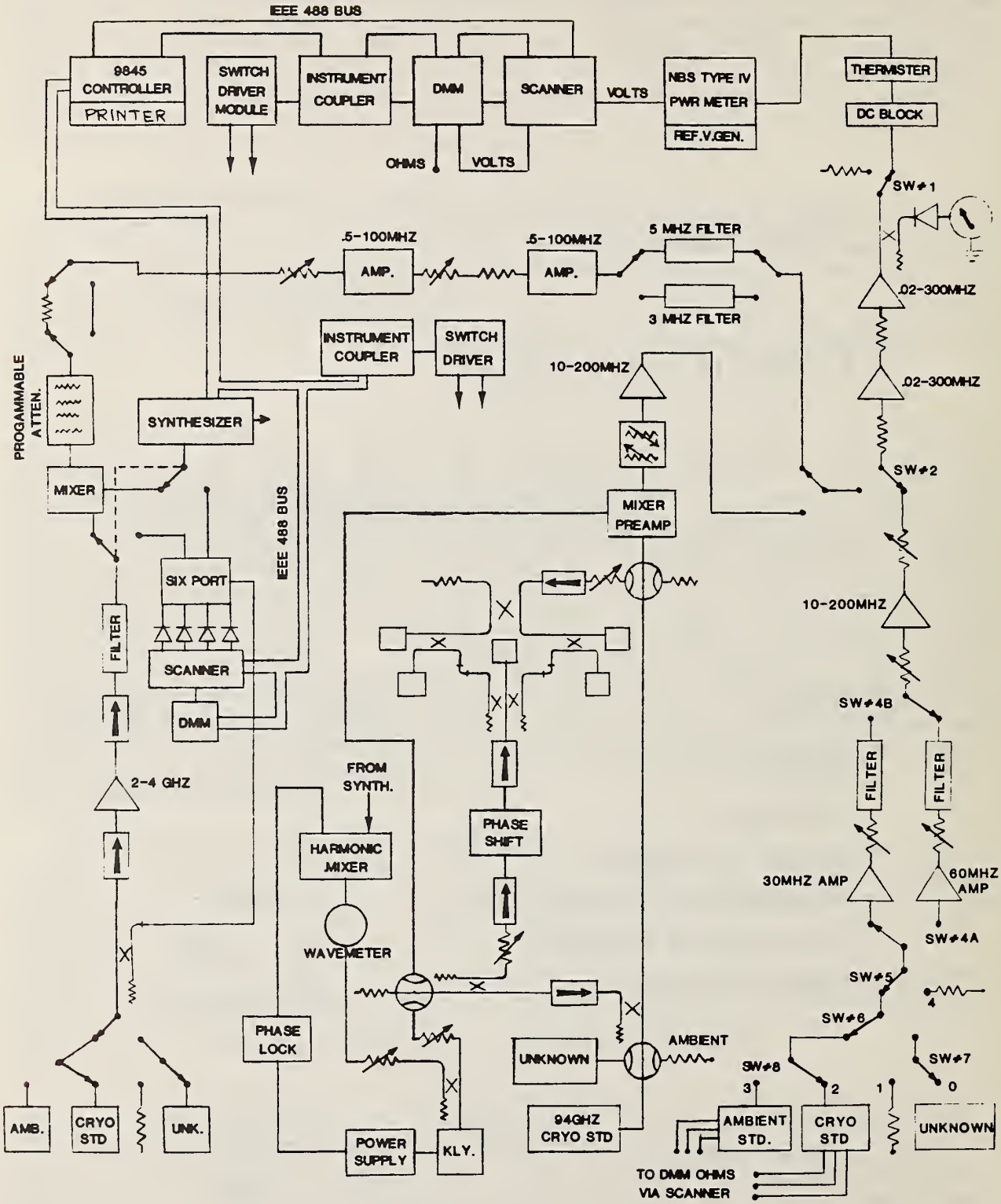

Figure 4. Current configuration of the automated radiometer.

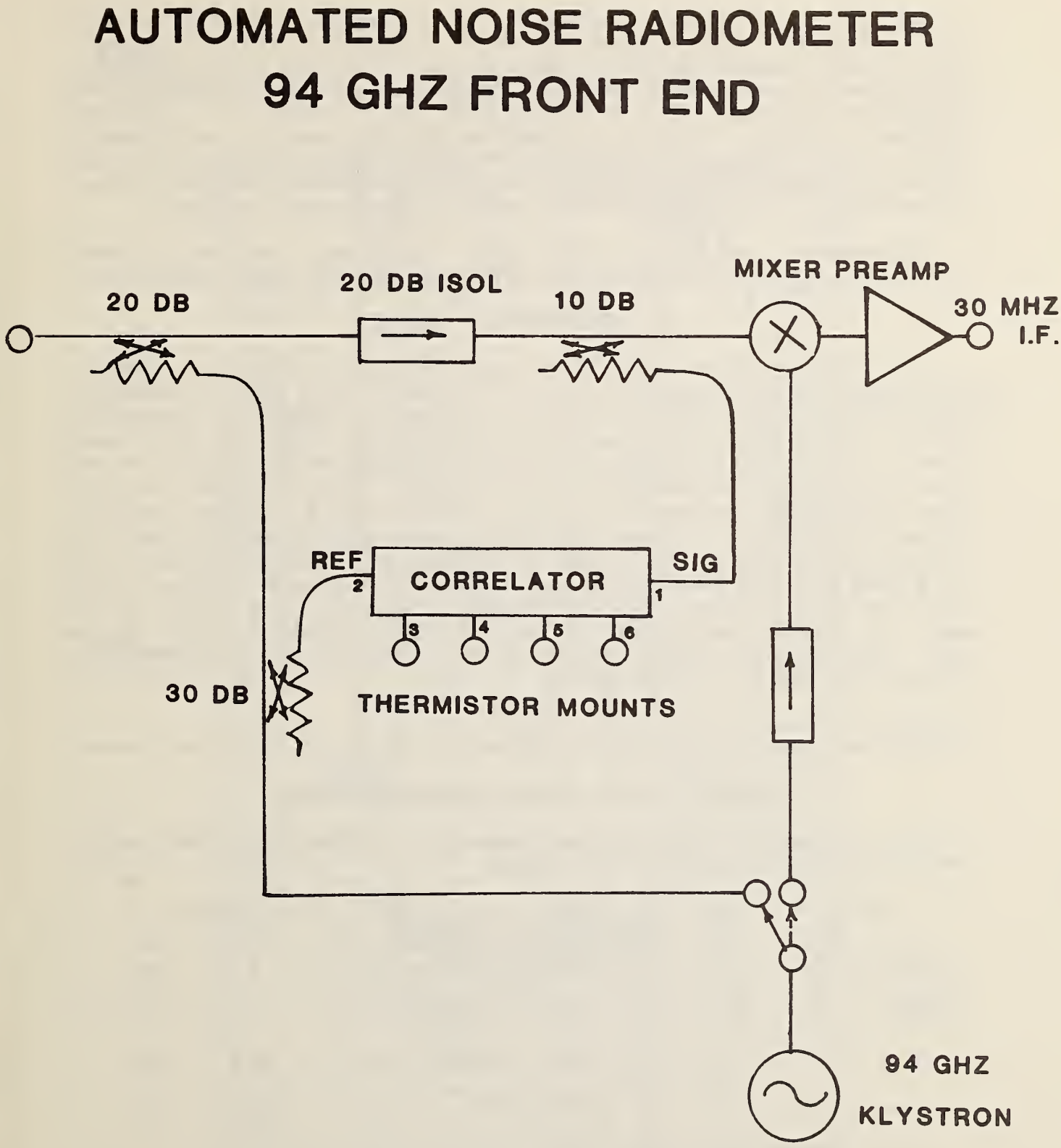

Figure 5. 94 GHz front end including six-port reflectometer.

is completed, physical noise standards will exist for all frequencies below 18 GHz (although the standard might need to be evaluated at the new frequency). Finally, for frequencies above 18 GHZ, a new type of primary standard has been developed which makes extensions to new frequency ranges relatively easy. The new standard consists of a millimeter wave horn "looking" at a cryogenic absorber, as shown in figure 6. Since the analysis used for one frequency range is easily extended to a different frequency range, and because the same evaluated cryogenic absorber can also be used for different frequency ranges, new standards can sometimes be created merely by constructing new horns.

To provide a new 20 GHz noise calibration service then requires three parts: a new horn noise standard, a 20 GHz front end, and a system evaluation.

3. MEASUREMENTS AT 20 GHZ

The characteristics of the Earth terminals that are being considered in this examination are shown in Table 2. For the 0.3 m (1 ft), 0.6 m (2 ft), 1.8 m (6 ft), and 2.4 m (8 ft) diameter antennas, the temperature rise at the output of the antenna due to the Sun or the Moon are listed for those cases where it is practical to correct for the finite extent of the source (referred to as the star shape correction factor) [2,28,30]. Table 2 indicates that the signal produced by the Moon is too small compared with T_{sys} except, perhaps, for the 2.4 m antenna. Further, Table 2 indicates that one cannot correct for the finite size of the Sun or Moon for antennas with diameters greater than 2.4 m, and only the Moon can be used with an 2.4 m diameter antenna. This last conclusion is rather important because it precludes the use of the Sun even as a transfer source and implies that only a satellite signal may be used. Because this is important and not immediately obvious, it is discussed in more detail before continuing on.

TABLE 2. Earth Terminals being Considered.

It is assumed that the system temperature is 1000 K and the aperture efficiency is 55% for each antenna system.

Ant. Diam		G/T	G	HPBW	SUN		MOON	
m	(ft)	(dB)	(dB)	(deg)	T(ant)	Y	T(ant)	Y
0.31	(1)	3.5	34	3.38	46 K	1.05	1 K	1.001
0.61	(2)	9.5	40	1.69	180 K	1.18	4 K	1.004
1.83	(6)	19.1	49	0.56	1380 K	2.38	31 K	1.031
2.44	(8)	21.6	52	0.42	-	-	48 K	1.053
6.10	(20)	29.5	60	0.17	-	-	-	-
13.72	(45)	36.6	67	0.08	-	-	-	-

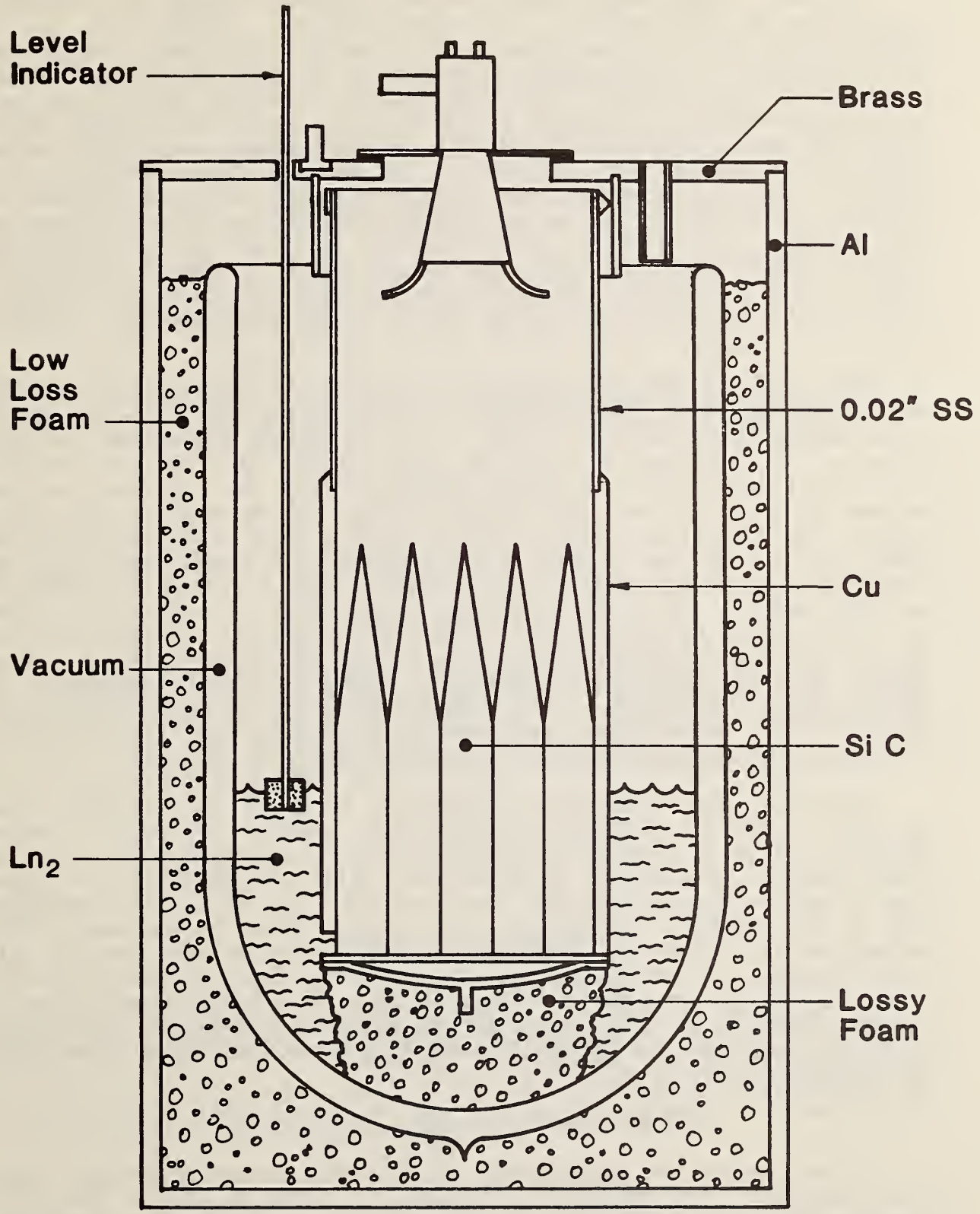

Figure 6. 94 GHz Cryogenic Noise Standard.

To obtain a star shape factor, one has to know or assume the brightness distribution of the source and the antenna pattern, calculate the source-antenna convolution, estimate the errors caused by the limitations in the distribution/pattern assumptions, and obtain a practical algorithm to represent this convolution integral for different antenna HPBW's, the frequency ranges desired, and source conditions (i.e., secular decay, Moon phase, Moon-Earth distance, etc.). In practice, the star-antenna convolution calculation results are not very dependent on the antenna pattern assumed nor the details of the star brightness distribution as long as the source is smaller than the antenna HPBW. That is, assuming that the antenna pattern is Gaussian does not give a significantly different result than using an actual measured antenna pattern; and assuming some appropriate, simple brightness distribution (e.g., a disk distribution with the "best" diameter and brightness) does not give a significantly different result than using the actual measured distribution.

This situation changes dramatically as the size of the source approaches and exceeds the HPBW of the antenna. Instead of the star shape correction factor depending on neither the details of the antenna pattern nor the star brightness distribution, it begins to depend heavily on both. For example, for a point source the star shape factor is unity and independent of the antenna pattern. For an ideal disk source equal to the HPBW of the antenna pattern, the star shape factor is near 0.7 and a 1% error in estimating the HPBW causes a 0.5% error in the star shape factor. For a disk source equal to twice the HPBW, the star shape factor is only 0.3 and a 1% error in estimating the HPBW causes a 1.6% error in the star shape factor. In principle, if one had an accurately measured antenna pattern and a detailed brightness map for the source, the appropriate star shape correction factor could be calculated. But this shifts the measurement from being an easy measurement to being a major undertaking. The antenna would have to be constructed or mounted so that the necessary measurements are feasible, and an adequate far-field source or adequate near-field measurement facility available.

Further, if the source size approaches or is larger than the HPBW, a new and very significant problem is encountered. Namely, (4) and (7) become inappropriate as κ (because of the star shape correction factor) becomes nearly inversely proportional to the receiver gain. The physics of the situation is that the magnitude of the signal "on star" (see eq 2) begins to depend only on the brightness temperature of the source and not on the shape of the antenna pattern. That is, if the antenna were defocused, the boresight gain would decrease, but the pattern widens so that the total radiation collected by the antenna is nearly the same (assuming that the brightness temperature of extended source is uniform). As κ becomes inversely proportional to G, the G dependence drops out, and the measurement error becomes unbounded (because NEF and G/T depend directly on G).

3.1 Measurements of Small Earth Terminals

In this section the accuracy and repeatability associated with two potential measurement techniques are estimated, (1) using the Sun or Moon as a known source, and (2) using the Sun or Moon as a transfer source. One could also use a satellite as a transfer source, as will be discussed in the next section for measuring G/T for large Earth terminals, and will not be discussed separately here.

3.1.1 Using the Sun or Moon as Known Sources

Figure 7 [45] shows a portion of a graph describing the magnitudes of the various sources of radiation in the solar atmosphere that contribute to the total solar radio emission. Superimposed on this graph are hash marks representing monthly-averaged measurements [46] of the solar output by the Air Force Geophysical Laboratory (AFGL) from January 1979 to May 1982 at 5, 8.8, and 15.4 GHz. It is clear that, as the frequency increases, the solar output is increasingly better approximated by the quiet-sun component alone. At 15.4 GHz the quiet-sun graph gives the solar output as 580 sfu (1 solar flux unit = 10^{-22}W/m^2/Hz/steradian) ± 60 sfu between the S.S. (sunspot) maximum and minimum curves. The average of the AFGL measurements for the period indicated is 566 sfu with about the same spread as the graph between max and min S.S. activity. The difference between the two averages (580 and 566) is 14 sfu, so it is reasonable to expect the average graph value to approximate the true solar output to within ±74 sfu (60 + 14). It is also reasonable to expect no larger error at 20 GHz. Therefore, it appears safe to assume that the solar output can be approximated by

$$853 \pm 74 \text{ sfu}$$

at 20 GHz, where 853 sfu is the average graph value at 20 GHz.

3.1.1.1 Solar Star-Shape Factor

At 20 GHz most of the solar radio emission comes from the region of the chromosphere [47] that is within 1% of the solar photosphere. This implies that to first order the brightness-temperature is approximately uniform across the solar disk, and appears to come from a circular disk with the same apparent diameter as the photosphere. For this model the star-shape factor is

$$k_2 = (1 - \exp(-x^2))/x^2 \tag{8}$$

where

$$x^2 = (\ln 2)\,(d/\text{HPBW})^2 \tag{9}$$

and where d is the optical angular diameter of the Sun subtended at the antenna site. The error in the preceding approximation has not, as yet, been analyzed and will be taken as zero for the present. The value for d can be easily obtained [48] to less than ±0.06%. The error in the HPBW depends on the technique used in viewing the Sun, and on the antenna. A graph of the resulting errors in k_2 is shown in figure 8.

3.1.1.2 Lunar Radio Emission

The lunar output equations developed for the 1 to 10 GHz frequency range [30] were reexamined for 20 GHz. The resulting lunar flux density is

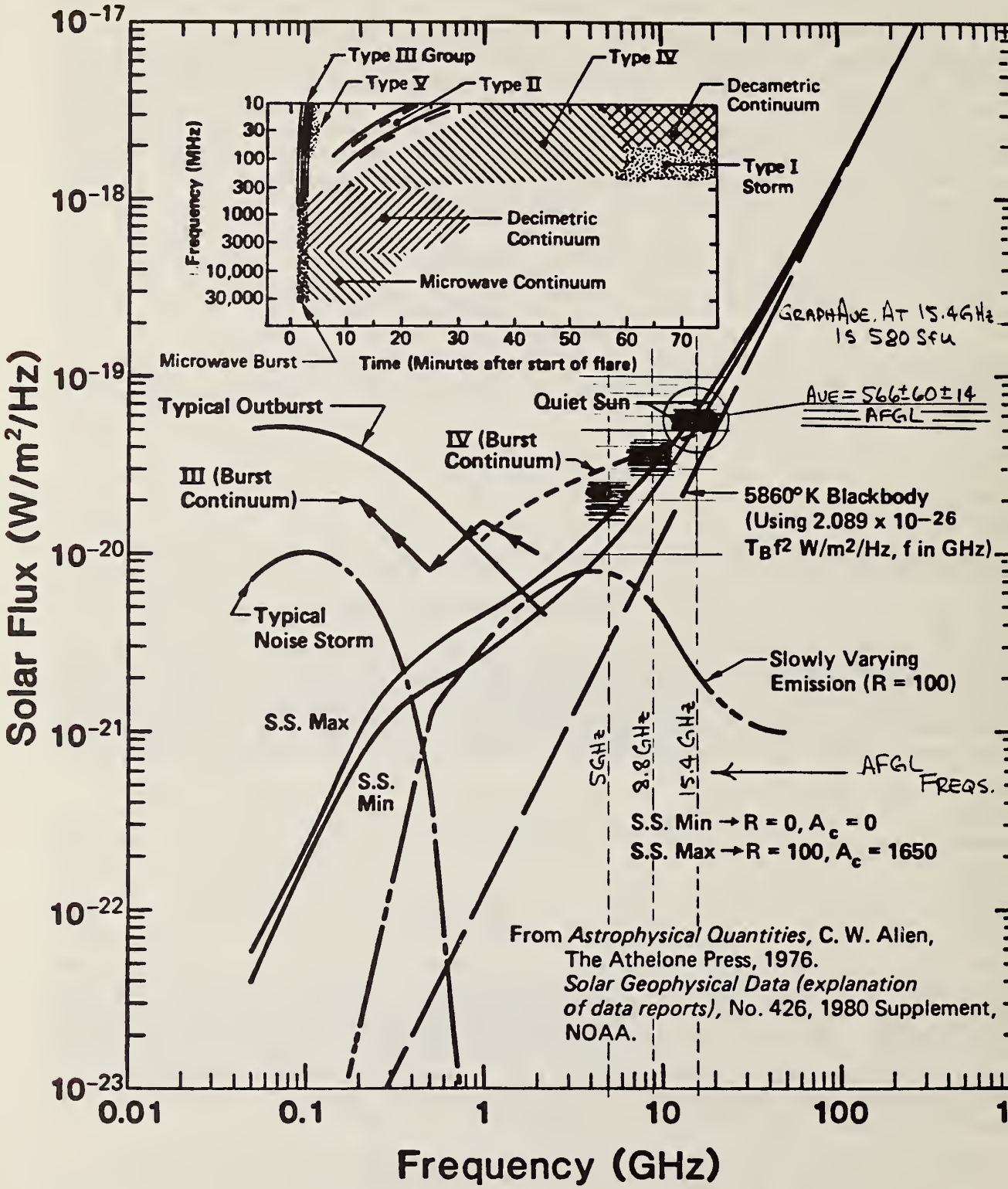

Figure 7. Solar radio emission.

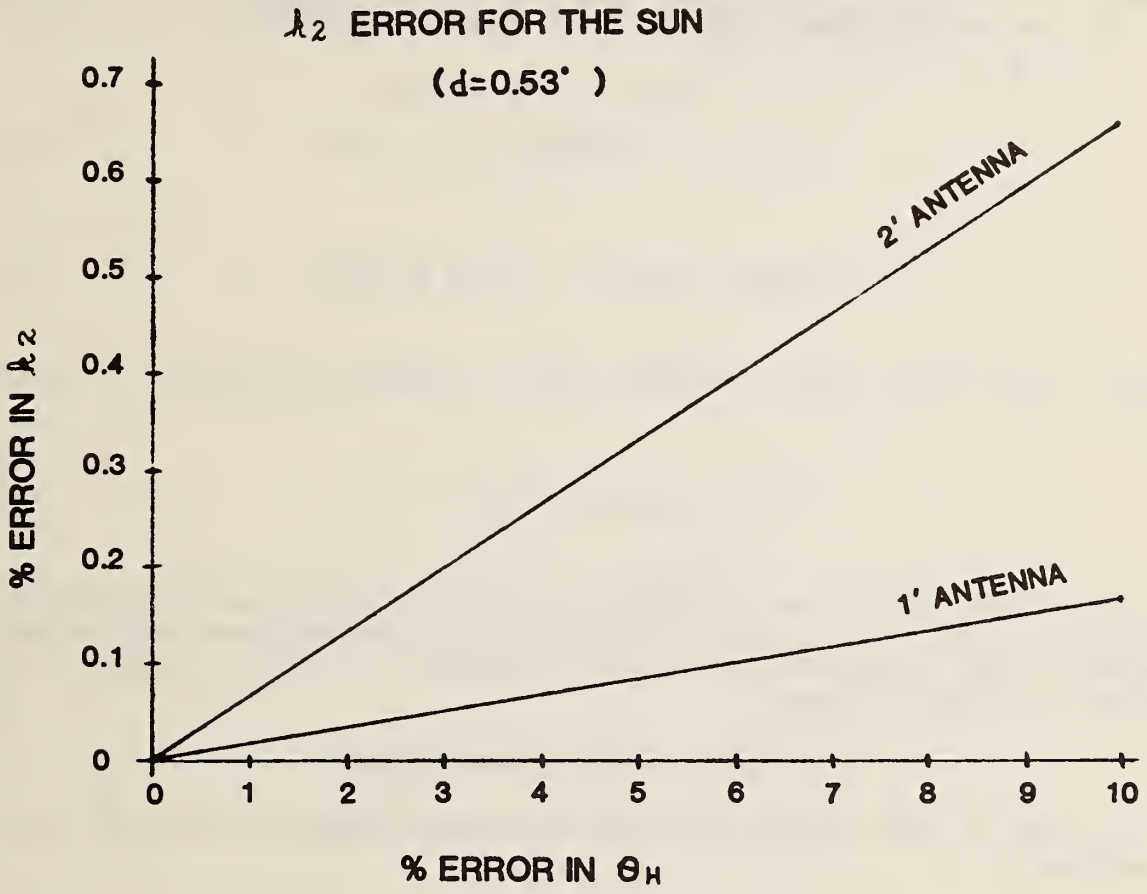

Figure 8. The k_2 error for the Sun.

$$S = 7.349\ f^2\ T\ d^2 \tag{10}$$

where, S is the flux density in janskys (10^{-26} W/m^2/Hz/steradian), f is the frequency in GHz, T is the average lunar brightness temperature in kelvins, and d is the angular lunar diameter in degrees subtended at the antenna site. T and d are calculated from

$$T = 206.8\ (1 - 0.1648\ \cos(\phi - 35)) \tag{11}$$

and

$$d = 0.5182/\ c/60.268 - 0.0166\ \sin(el) \tag{12}$$

ϕ is the lunar phase angle in degrees, and is related to the phase F by the equation

$$\phi = \arccos(1 - 2F). \tag{13}$$

F can be obtained [48] to an uncertainty of ±2% by a simple parabolic fit over a three-day period. The Earth-Moon separation (c) distance and is obtainable to within ±0.02% by the same procedure. The error in S due to these various parameters is given in Table 3.

3.1.1.3 Lunar Star-Shape Factor

The 1 to 10 GHz analysis [30] leads to the following star-shape factor for the Moon:

$$k_2 = (1 - \exp(-x^2)/x^2) \pm 0.65\%, \tag{14}$$

where

$$x^2 = 0.6455\ (d/HPBW)^2. \tag{15}$$

The 0.65% is the minimum error in k_2 due to the approximate nature of the disk model, and the constant 0.6455 was chosen to minimize this error. The apparent angular diameter (d) of the Moon subtended at the antenna site and can be obtained from (12) to within ±0.1%. Including this error with the 0.65% error leads to the k_2-error-versus-HPBW error shown in figure 9. The graph was prepared for an eight-foot antenna (assuming a 0.43 degree HPBW).

3.1.1.4 Water Vapor and Molecular Oxygen

There is attenuation of radio waves at 20 GHz caused by the absorption due to water vapor and due to molecular oxygen. The first water-vapor resonance line lies at 1.35 cm (22.2 GHz), and is close enough to 20 GHz to

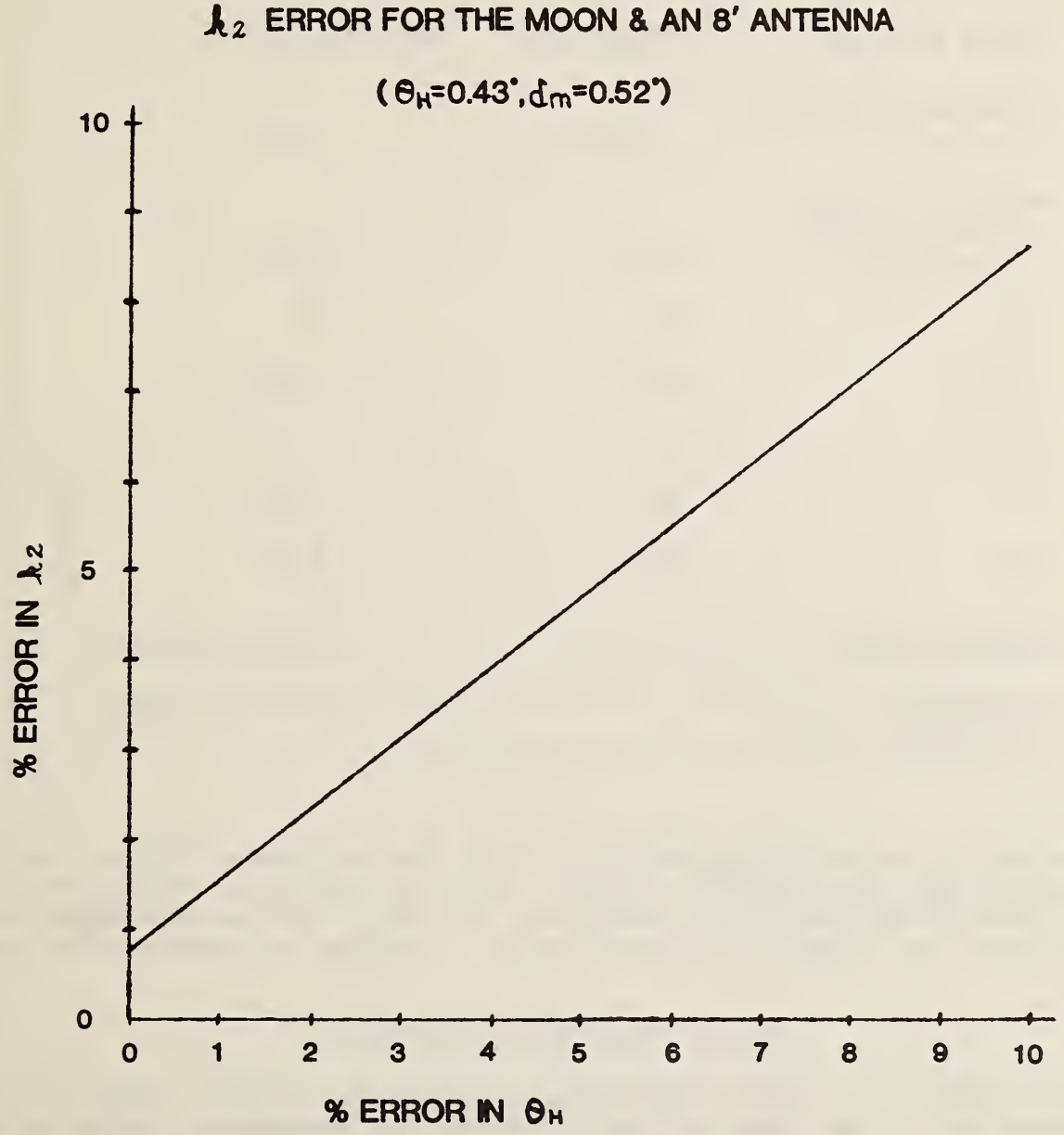

Figure 9. The k_2 error for the Moon and a 2.4 m antenna.

cause serious errors in the algorithms developed for the 1 to 10 GHz system. These algorithms were therefore modified by approximating a collision term in

TABLE 3. Systematic Lunar Flux Density Errors at 20 GHz.

Source of Error	Magnitude	Resulting % Error in S
Variation in the Solar Insulation	3.34% + 1%	4.34
Neglect of Higher Harmonics in the lunar phase.	0.61%	0.61%
To	5%	5%
T_1/T_o	6.6%	1.09%
cos ϕ	0.04	0
Ψ	5%	0.50%
d	0.1%	0.2%
Quadrature Sum		6.76% (0.28 dB)
Linear Sum		11.7% (0.48 dB)

the denominator of the absorption coefficients that was ignored in the 1 to 10 GHz version (to save computation time). With the addition of this term, the total error in the atmospheric efficiency "a" due to gaseous absorption was recalculated and appears in figure 10 as a function of antenna elevation angle.

3.1.1.5 Atmospheric Refraction

The decrease in radio refractivity with altitude causes a spreading in the wavefront of any radiation coming through the atmosphere, leading to a decreased flux density and, consequently, an effective attenuation. However, there is no significant difference in this attenuation between 10 and 20 GHz. The present algorithms are, therefore, sufficient to account for this effect.

3.1.1.6 Diffusive Attenuation

Tropospheric turbulence causes a diffusion of rays, and a distortion of the resulting wavefront over the antenna aperture. Both effects effectively

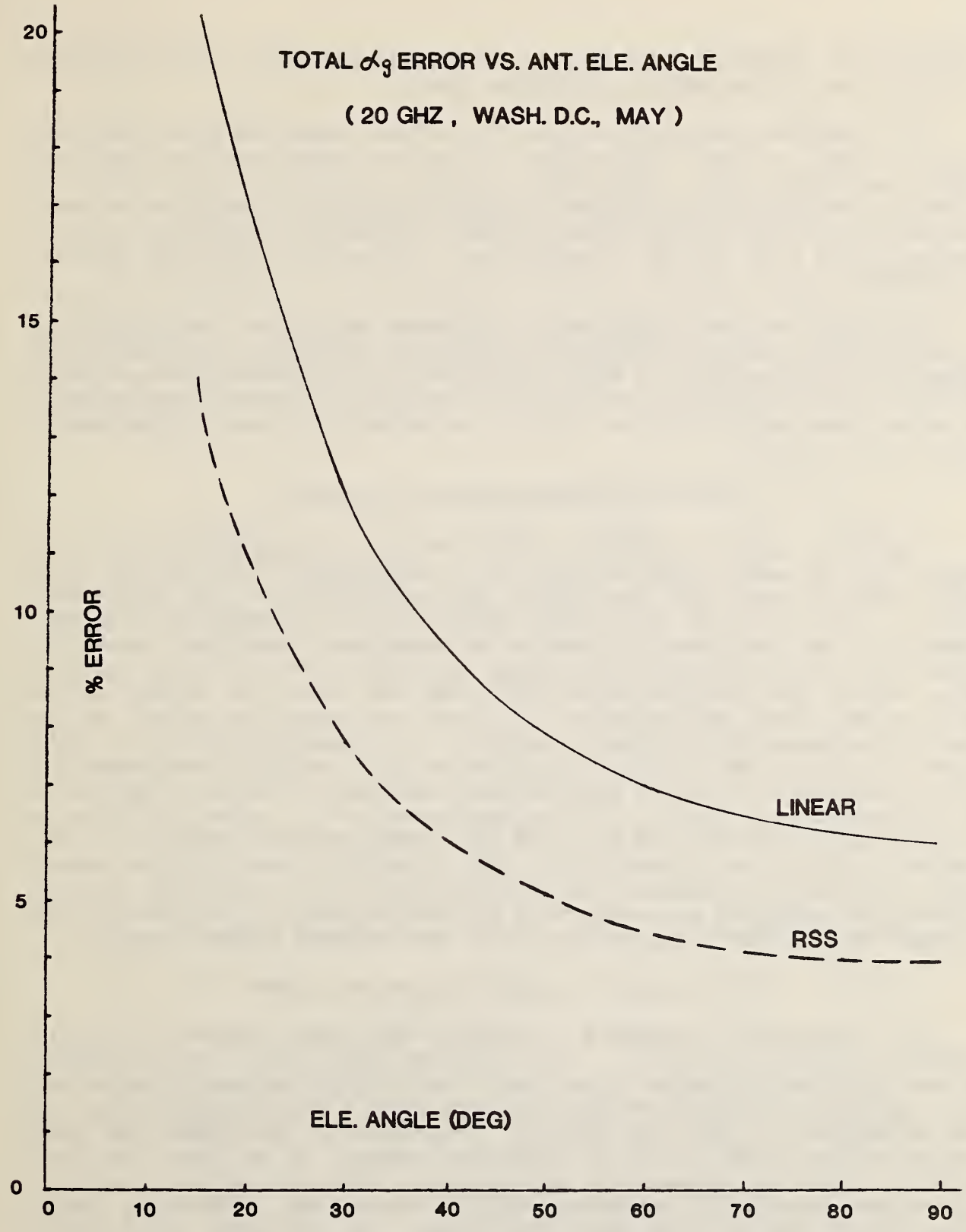

Figure 10. Total α_g error vs. antenna elevation angle.

attenuate the signal received through the antenna waveguide lead, and may be as significant as the gaseous attenuation itself.

The algorithms developed for the 1 to 10 GHz range were based upon some work by Yokoi, et. al., [37] which, in turn, was based upon the theory of Booker and Gordon [49]. This theory assumed a correlation function for the turbulence whose value is incapable of being extrapolated from the measurement frequencies of Yokoi to the 20 GHz of present interest, and since there is no available data at 20 GHz for transatmospheric attenuation, some other approach is needed.

The theory of wave propagation in a turbulent medium has been extensively developed [50], and with the numerous clear-air turbulence measurements, it appears possible to obtain a useful estimate of the effective attenuation at 20 GHz. However, this task will require an additional effort which could not be accomplished with the current funding, so reliable estimates are not available for this report.

3.1.1.7 Estimated Measurement Accuracy

The best accuracy attainable using the Sun or the Moon directly to measure G/T of small Earth terminals is an uncertainty of about ±40% (±1.5 dB). Table 4 summarizes the sources and contributions of the measurement errors. Because (1) the measurement techniques are elaborate and time consuming, (2) the conditions for meeting the measurement conditions needed for Table 4 are rather stringent and, thus, expensive in time and money to produce, and (3) the resulting errors are large, the direct use of the Sun or Moon for the primary measurement of G/T is not very attractive and will not be further considered in this report. However, the recommendation (later in this report) is to use the Sun as a known source for a secondary measurement of G/T. From Table 4, it can be seen that the atmospheric effects are the source of the large error. Thus, if in the measurement of G/T, using the Sun as a transfer source, the data are also used to see what G/T would have been if the Sun had been used as a known source, then information concerning the atmospheric loss can be presented. But more important, for "good" measuring conditions, the secondary measurements of G/T can be used to alert the operator if something happened to the calibration of the reference antenna system.

3.1.2 Using a Calibrated Comparison Antenna

An experimental arrangement to measure the system noise in an Earth terminal is shown in figure 11. The calibrated Earth terminal can be similar to the uncalibrated terminal except that a calibrated directional coupler and noise add reference source are inserted between a 0.6 m calibrated antenna and the preamplifier of the Earth terminal. The output of the system under test and the output of the calibrated system are connected to the ETMS. The ETMS switches alternately between the two terminals. The gain drift in the calibrated Earth terminal is compensated for by injecting the noise from a stable noise source into the front end of the system. The gain drift in the Earth terminal under test is compensated for by comparing its output with that of the calibrated Earth terminal.

TABLE 4. Estimated Accuracy in using the Sun or Moon.

The measurements are assumed to be made at 20 GHZ, at an antenna elevation of 15 degrees, a site elevation of 0.15 km, ambient temperature 80° F, dew point 46° F, and 0.1% noise power measurements. It is assumed that the earth terminals under test are gain stable within 0.5% over five minutes, or that it is equipped with a directional coupler at the front end of the terminal so that a noise add technique can be used to correct for the gain instability.

	|-----ERROR CONTRIBUTION TO G/T-----|		
Source Antenna Diameter	Sun 0.3 m	Sun 0.6 m	Sun 1.8 m	Moon 2.4 m
Parameter				
1. Flux	8.7 %	8.7 %	8.7 %	8.6 %
2. Y-factor (±0.1 %)	2.3 %	0.7 %	0.2 %	2.2 %
3. ET stability (±0.5 %)	11.5 %	3.3 %	0.9 %	11.0 %
4. Atmospheric absorption	29.0 %	29.0 %	29.0 %	29.0 %
5. Diffusive attenuation	30.0 ? %	30.0 ? %	30.0 ? %	30.0 ? %
6. Refractive attenuation	0.1 %	0.1 %	0.1 %	0.1 %
7. "Star" shape	0.1 %	0.1 %	0.2 %	4.4 %
8. Antenna point(±0% HPBW)	2.6 %	2.6 %	2.6 %	2.6 %
9. Antenna polarization	0.4 %	0.4 %	0.4 %	0.4 %
Linear sum	84.7 % (2.6 dB)	74.9 % (2.4 dB)	72.1 % (2.4 dB)	88.3 % (2.8 dB)
Quadratic sum	44.3 % (1.6 dB)	42.8 % (1.5 dB)	42.7 % (1.5 dB)	44.4 % (1.6 dB)

3.1.2.1 Measurement Method.

Both the test antenna and the calibrated antenna are pointed at the Sun (or Moon), then at the cold sky at the same elevation and the appropriate Y-factors (see (1)) are established for each Earth terminal. The respective G/T's are related to the associated Y-factors, Sun flux (or Moon flux), and atmospheric parameters, star shape factor, antenna polarization effects, etc. as implied in (4). Taking the ratio of the G/T for the unknown to the G/T for the calibrated system, one obtains,

$$(G/T)_x \simeq (Y_x - 1)/(Y_{std} - 1)\ (G/T)_{std} \tag{16}$$

where the subscript x refers to the Earth terminal under test, and the subscript std refers to the calibrated Earth terminal. Equation (16) is approximate in that the "star" shape factors, the antenna pointing, and the antenna polarization might differ slightly.

Using (16), $(G/T)_x$ is known when $(G/T)_{std}$ is determined. The antenna gain and the noise injected into the calibrated terminal by the noise add source are assumed to be calibrated by NBS. The system noise, T_{std}, which depends on the atmospheric conditions present at the field site, is determined using the calibrated injected noise, T_a. With the antenna of the calibrated Earth terminal pointed at the appropriate elevation angle, the ratio of the power out of the terminal with the noise add source on to when it is off is,

$$Y' = (T_{std} + T_a)/T_{std} \tag{17}$$

or

$$T_{std} = T_a/(Y' - 1). \tag{18}$$

Using G from a prior NBS calibration divided by T_{std} using (18) provides $(G/T)_{std}$ needed in (16).

Similarly, using (7) instead of (4) one obtains

$$NEF_x \simeq (Y_x - 1)/(Y_{std} - 1)\ (NEF_{std} + T_{sky}/A_{eo,std}) - T_{sky}/A_{eo,x} \tag{19}$$

where T_{sky} is estimated using the temperature, humidity, antenna pointing, and site altitude information [35]; and A_{eo} is estimated on the basis of the antenna diameter. Without a noise add technique available on the Earth terminal being measured, one can not make a direct measurement of T_{sky} or A_{eo}.

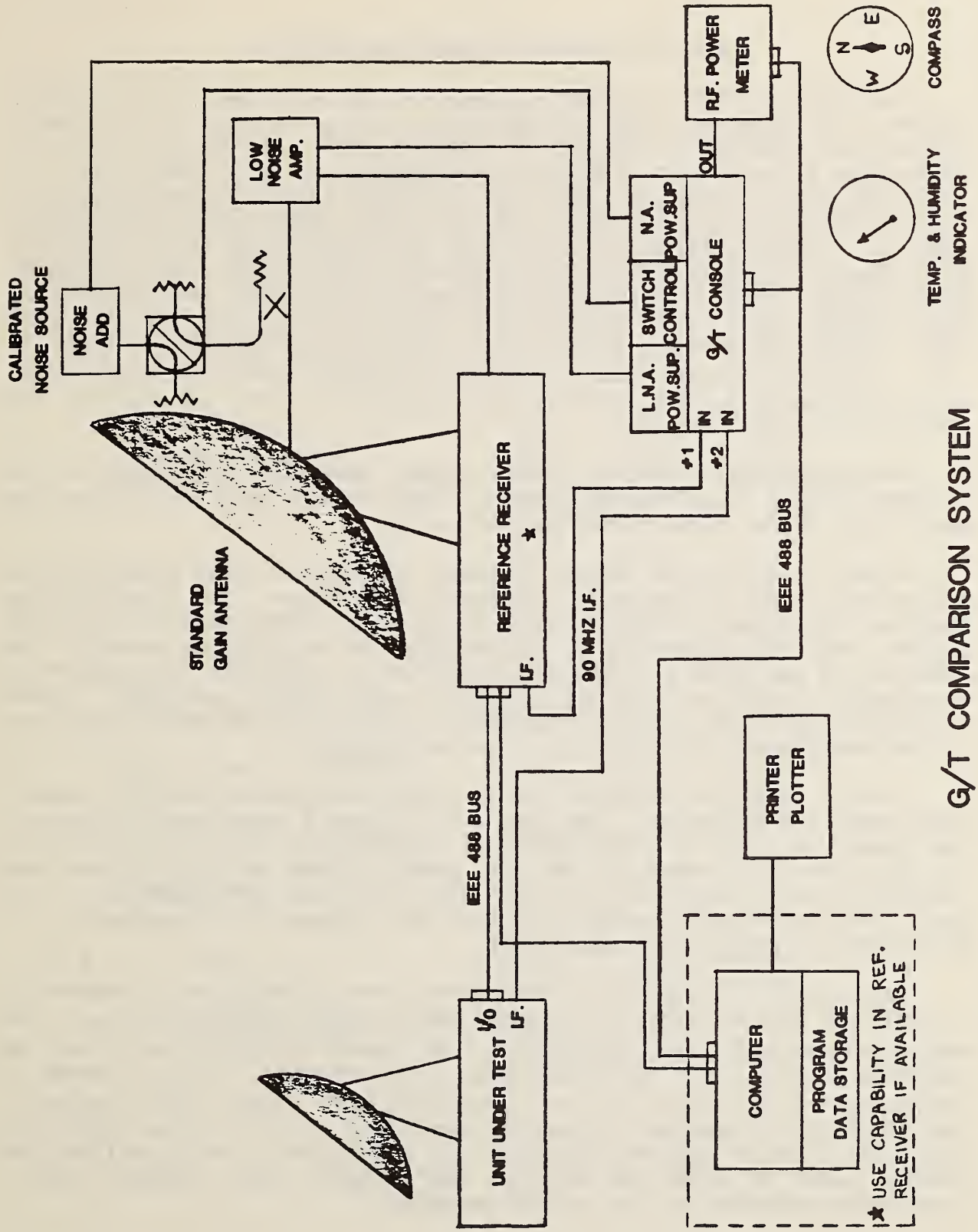

Figure 11. Experimental setup for G/T comparison measurement.

3.1.2.2 Estimated Measurement Accuracy

The estimate of the accuracy of measuring G/T of a small Earth terminal depends on many factors. The optimum choice depends, in part, on the size of the antenna system under test, and the cost-accuracy trade off that suits the needs. For a test measuring system that minimizes the measurement error, G/T can be measured to about ±0.3 dB. The sources of error, and their contribution to the total error for this "best" G/T measurement system are shown in Table 5. From Table 5, the error that dominates is the uncertainty with which the G/T of the reference Earth terminal is known. Thus, from a measurement point of view, it pays to put the measurement effort into calibrating this reference terminal. In particular, Table 5 assumed the use of a 0.1% power ratio measurement so that $(Y_{std} - 1)$ error contributed 1% error to G/T. This table suggests that the use of a 0.5% power ratio measurement might not significantly degrade the measurement accuracy for the 1.2 m (4 ft) and 1.8 m (6 ft) Earth terminals.

The measurement errors in Table 5 assume that the noise source in the measuring system is calibrated against a WR42 primary noise standard by the NBS, which, at the present time, does not exist.

Without a calibration service, probably the best one could do would be to assume the output of an argon gas discharge noise source. Our experience has been that for properly designed, properly cared for argon gas discharge noise sources, most are within 15% of the predicted values, but not always. The tubes do age and do have a finite usable lifetime. Without a good comparison radiometer, it would be difficult to identify which tube is going bad. To use an uncalibrated noise source in a measuring system is too serious a compromise to the measurement and, therefore, is not recommended.

Table 6 shows the impact on the quadrature measurement error for several measurement system options. The first line in Table 6 corresponds to the system assumed for Table 5. From Table 6 we see that by using a 0.5% power meter in measuring G/T instead of the 0.1% meter assumed in Table 5 does not increase the error very much for the 2 foot or 6 foot Earth terminals. For the 1 foot Earth terminal, the 0.5% power meter causes the measurement error to increase to about 0.59 dB uncertainty.

Also shown in Table 6 is the resulting error in measuring G/T depending on different uncertainties for the noise source used to measure $(G/T)_{std}$. The most accurate measurements of G/T (±0.3 dB) assume the noise source used to determine $(G/T)_{std}$ was calibrated with an uncertainty of 2% (assuming a calibration service based on a yet unavailable WR42 primary noise standard). The accuracy of measuring G/T degrades about 0.05 dB if the noise source was calibrated with an interim standard to an uncertainty of 4% (a calibration service based on using the existing WR62 primary noise standard with a calibrated transition section to WR42 waveguide).

TABLE 5. "Best" G/T Accuracy for Small Terminals.

This table lists errors anticipated in measuring G/T using the comparison method with a measurement system which minimizes the resultant error. The errors listed are those associated with the uncertainty in the parameter indicated. It is assumed that the reference terminal has a 0.6 m (2 ft) calibrated antenna, both antennas are pointed at the same source within 10% of their half-power beamwidths, the system temperatures are 1000 K, and the ETMS-1 uses a noise source calibrated within 2% against a WR42 primary noise standard and measures noise power ratio with an uncertainty of 0.1%.

Source antenna diameter	Sun 0.3 m	Sun 0.6 m	Sun 1.8 m
parameter	error in G/T		
$(Y_x - 1)$	2.3 %	0.7 %	0.2 %
$(Y_{std} - 1)$	0.7 %	0.7 %	0.7 %
$(G/T)_{std}$	5.0 %	5.0 %	5.0 %
"star" shape (unknown)	0.1 %	0.1 %	0.2 %
"star" shape (calibrated)	0.1 % 2.6 %	0.1 % 2.6 %	0.1 % 2.6 %
antenna point calibrated	2.6 %	2.6 %	2.6%
antenna polarization	0.4 %	0.4 %	0.4 %
Linear error	13.8 % (0.56dB)	12.2 % (0.50dB)	12.1 % (0.49dB)
Quadrature error	6.7 % (0.28dB)	6.3 % (0.27dB)	6.3 % (0.26dB)

TABLE 6. Measurement Accuracy Options for small terminals.

This table lists the total quadratic errors anticipated in measuring G/T using different measuring system specifications. The measurement system options are (a) to use an NBS type IV power meter with 0.1% uncertainty, or a commercial power bridge with 0.5% uncertainty, and (b) to use a noise source in the measuring system calibrated with an accuracy of 2% using a new WR42 primary noise standard, or a noise source calibrated with an accuracy of 4% using an existing WR62 primary noise standard with a calibrated transition section. In all cases, it is assumed that the reference Earth terminal has a 0.6 m diameter antenna that can be pointed to within 10% of its HPBW and a 1000 K system noise. All measuring systems use a comparison method with the Sun as the transfer source.

(Source) (Antenna diameter of unit under test)		Sun 0.3 m	Sun 0.6 m	Sun 2.4 m
noise pwr meas accuracy	noise calbr accuracy	quadratic error to G/T		
0.1%	2%	0.28 dB	0.27 dB	0.26 dB
0.1%	4%	0.35 dB	0.33 dB	0.33 dB
0.5%	2%	0.51 dB	0.32 dB	0.29 dB
0.5%	4%	0.55 dB	0.37 dB	0.35 dB

3.2 Measurements of Large Earth Terminals

Neither the Sun nor Moon can be used as a transfer source for antennas larger than 2.4 m (8 ft). As the antenna size gets larger and larger, the output from the antenna depends less and less on the antenna gain, and more and more on only the brightness temperature of the source. At 20 GHz, the HPBW of the 2.4 m antenna is smaller than the Moon diameter and the sensitivity of the measurement using the Moon as a transfer source is marginal. Thus, for the larger antennas one is forced to use a satellite signal for the transfer source. The satellite signal provides better signal to noise, and it is polarized. The polarization match between the satellite signal and the receiving antennas are important, but it has been assumed that this is not a significant problem. If it is, this is better checked separately using techniques not addressed in this report.

The estimated uncertainty in measuring G/T for large Earth terminals is about 0.4 or 0.5 dB as noted in Table 7. It is assumed that a satellite signal is used for the measurement transfer signal. From Table 7, one can see that the error contributions from the various sources are about the same magnitude, implying that the measurement assumptions for this table are near "optimum." Thus, for example, it is clear that the expense of using a 0.1% power bridge is justified if the satellite signal to noise is 10:1 for a 13.7 m (45 ft) Earth terminal as assumed (because a 0.5% power bridge would cause 5 times the errors listed for $(Y_x - 1)$ and $(Y_{std} - 1)$, and the resulting 18% error for $(Y_{std} - 1)$ would completely dominate the error budget). On the other hand, if satellite signal-to-noise ratios of 50:1 are readily available, then a 0.5% power bridge would be more "optimum". The question marks next to some of the error listings are a reminder that the estimate of the magnitude of the diffusive attenuation is rather uncertain. More theoretical work on the diffusive attenuation problem is a must for the G/T measurements of large Earth terminals.

TABLE 7. G/T Comparison Accuracy for Large Terminals.

This table lists typical errors anticipated in measuring G/T using the comparison method. It is assumed that the source used in the comparison is a satellite and the signal to noise available for a 13.7 m (45 ft) Earth terminal is 10:1. The errors listed are those associated with the uncertainty in the parameter indicated. It is assumed that the Earth terminal being tested has a directional coupler in front of the preamplifier where a noise add signal can be injected in order to correct for changes in gain. It is also assumed that the calibration terminal has an 2.4 m calibrated antenna, the system temperature is 1000 K, the noise source in the reference Earth terminal is calibrated to an uncertainty of 2%, the antenna can be pointed to the satellite within 10% of its HPBW, and the power is measured with an uncertainty of 0.1%.

antenna diameter	2.4 m	6.1 m	13.7 m
parameter		error in G/T	
$(Y_x - 1)$	3.6 %	0.6 %	0.1 %
$(Y_{std} - 1)$	3.6 %	3.6 %	3.6 %
$(G/T)_{std}$	5.0 %	5.0 %	5.0 %
diffusive attenuation	0. %	3.0 %?	10.0 %?
antenna point unknown	2.6 %	2.6 %	2.6 %
antenna point calibrated	2.6 %	2.6 %	2.6 %
antenna polarization	0.4 %	0.4 %	0.4 %
Linear error	17.8 % (0.7 dB)	17.8 %? (0.7 dB)	24.3 %? (0.9 dB)
Quadrature error	8.0 % (0.3 dB)	7.8 %? (0.3 dB)	12.3 %? (0.5 dB)

4. RECOMMENDATIONS AND CONCLUSIONS

In this section, what measurement technique and system are most likely to meet the needs for future 20 GHz satellite systems are considered.

For measuring G/T of small Earth terminals, two different systems should be considered; (1) an Earth Terminal Measuring System (ETMS-1) constructed similarly to the existing ETMS shown schematically in figure 1 (with measurement accuracy of 0.3 dB or better using a gain comparison technique with the Sun/Moon as the transfer source), and (2) an Earth Terminal Measuring System (ETMS-1a) similar in purpose to the ETMS-1 but simplified by using a 0.5% power ratio measurement. If the 0.5 dB measurement uncertainty for the 0.3 m (1 ft) terminal is adequate, the simpler ETMS-1a is preferred (about 0.35 dB uncertainty for the 0.6 m (2 ft) and 1.8 m (6 ft) systems). A potential advantage of the ETMS-1a is that an existing computer within the reference Earth terminal might be utilized (provided it has an IEEE 488 port that can be used as a controller, some means of entering the G/T comparison program exists, and hard copy output is available).

Due to the uncertainty (see Table 4) and complexity, it is not recommended to use the Sun or Moon directly for the primary measurement of G/T. However, this method is recommended as a secondary measurement. That is, by using the known flux value of the Sun, and reusing the the Y-factor data obtained in the comparison measurement, an independent measurement of G/T is available. From this redundant measurement one can either deduce the atmospheric loss, or verify that the reference terminal is holding calibration. Furthermore, as a secondary measurement, the elaborate star drift measurements and the sophisticated data fitting routines are avoided, albeit additional theoretical work concerning the diffusive attenuation by the atmosphere is needed. A bonus for completing the diffusive attenuation theory is that the calculation of NEF (discussed in section 2) can also be implemented without any great effort.

For measuring G/T of large Earth terminals (antenna diameters greater than 1.8 m (6 ft), it is necessary to use a G/T comparison technique which utilizes a satellite signal as the transfer source. Unless signal-to-noise ratios substantially greater than 10:1 are available for the 13.7 m (45 ft) diameter antenna systems, then one needs to use a measuring system, ETMS-2 which incorporates an uncertainty of 0.1% accuracy noise-power-ratio meter.

ACKNOWLEDGMENTS

The authors wish to acknowledge the helpful discussions of John Wakefield and the financial support of the U.S. Army Communications Electronics Command, Fort Monmouth, New Jersey.

REFERENCES

[1] Wait, D. F. Satellite Earth Terminal G/T Measurements. Microwave J.: 49-58; 1977 April.

[2] Wait, D. F.; Daywitt, W. C.; Kanda, M.; Miller, C. K. S. A study of the measurement of G/T using Cassiopeia A. Nat. Bur. Stand. (U.S.) NBSIR 74-382; 1974 June. 187 p.

[3] Kochevar, H. J. Measurements of Earth station antennas G/T ratio by radio stars and satellites. Progress in astronautics and aeronautics, an American Institute of Aeronautics and Astronautics Series, Martin Summerfield, Series Editor, Vol. 33, Communications Satellite Technology, Edited by P. L. Bargellini; 1974. 359-370.

[4] Sion, A. New method for direct G/T measurement using satellite signals. Electron. Lett., Vol. 17, No. 23; 1981 November 12.

[5] Crane, W. S.; Pickett, R. B. Impact of solar calibration on telemetry system testing and checkout. International telemetering conference; 1972 October 10-12; International Hotel, Los Angeles, Calif. Sponsored by IFT. 584-590 [27]. C.C.I.R. (International Radio Consultative Committee), Earth-station antennae for the fixed satellite service. XIIIth Plenary Assembly, Geneva, 1974. Vol. IV, Fixed service using communication satellites (Study Group 4), Report 390-2; 160-176.

[6] C.C.I.R. (International Radio Consultative Committee). Earth-station antennae for the fixed satellite service. IIIth Plenary Assembly, Geneva, 1974; Vol. IV, Fixed service using communication satellites (Study Group 4), Report 390-2; 160-176.

[7] IEEE standard definitions of terms for antennas. IEEE Standard 145-1973, 1972 August 2.

[8] Methods of measurement for radio equipment used in satellite Earth stations, Part 3: Methods of measurement for combinations of sub-systems, Section 2: Measurement of the figure of merit G/T of the receiving system in the 4 GHz to 6 GHz range. International Electrotechnical Commission, IEC Standard, publication 510-3-2, Bureau Central de la Commission Electrotechnique Internationale, 1, rue de Varembe', Geneve, Suisse.

[9] Kreutel, R. W., Jr.; Pacholder, A. O. The measurement of gain and noise temperature of a satellite communications Earth station. Microwave J. 12(10): 61-66; 1969 October.

[10] Mattes, J. E. Verification of the figure of merit of Earth stations for satellite communications. Proceedings of the IREE, 1973 April; Vol. 61, No. 4. 77-84.

[11] Satellite communications reference data handbook. Defense Communications Agency (NTIS AD-746165), Washington, D.C. 20305; 1972 July. 385 p.

[12] Wait, D. F. Earth terminal measurement system operations manual. Nat. Bur. Stand. (U.S.) NBSIR 78-879; 1978 April. 261 p.

[13] Bathker, D. A. Radio-frequency performance of an 85-ft ground antenna: X-band. Technical Report 32-1300, National Aeronautics and Space Administration, Jet Propulsion Laboratory, California Institute of Technology, Pasadena, Calif. 1968 July 1. 34 p.

[14] Bathker, D. A. Radio frequency performance of a 210-ft ground antenna: X-band. National Aeronautics and Space Administration Technical Report 32-1417, Jet Propulsion Laboratory. 1969 December 15. 25 p.

[15] Benjauthrit, B.; Mulhall, B. D. L. X-band antenna gain and system noise temperature of 64-meter deep space stations. National Aeronautics and Space Administration, Deep Space Network Progress Report 42-39, Jet Propulsion Laboratory. 1977 March-April. 76-99 p.

[16] Kanda, M. Accuracy considerations in the measurement of the power gain of a large microwave antenna. IEEE Trans. Antennas Propagat., Vol. AP-23, No. 3: 407-41; 1975 May.

[17] Curry, W. H. Antenna-performance measurements using celestial sources. Ham Radio Magazine, 10th Annual Antenna Issue: 75-79; 1979 May.

[18] Kerns, D. M. Correction of near-field antenna measurements made with an arbitrary but known measuring antenna. Electron. Lett., Vol. 6, No. 11: 346-347; 1970 May 28.

[19] Newell, A. C. Determination of both polarization and power gain of antennas by a generalized 3-antenna measurement method. Electron. Lett., Vol. 7, No. 3: 68-70; 1971 Feb. 11.

[20] Kerns, D. M. New method of gain measurement using two identical antennas. Electron. Lett., Vol. 6: 348-349; 1970 May 28.

[21] Newell, A. C.; Baird, R. C.; Wacker, P. F. Accurate measurement of antenna gain and polarization at reduced distances by an extrapolation technique. IEEE Trans. Antennas Propagat., Vol. AP-21: 418-431; 1973 July.

[22] Schuster, D.; Stelzried, C. T.; Levy, G. S. The determination of noise temperatures of large paraboloidal antennas. IRE Trans. Antennas Propagat., Vol. PGAP-10, No. 3: 286-291; 1962 May.

[23] Engen, G. F. A new method of characterizing amplifier noise performance. IEEE Trans. Instrum. Meas., Vol. IM-19, No. 4: 344-349; 1970 November.

[24] Wait, D. F. Considerations for the precise measurement of amplifier noise. Nat. Bur. Stand. (U.S.) Tech. Note 640; 1973 August 1. 29 p.

[25] Wait, D. F. Thermal noise from a passive linear multiport. IEEE Trans. Microwave Theory and Techniques, Vol. MTT-16, No. 9: 687-691; 1968 September.

[26] Hedeman, W. H. The Sun as a calibration signal source for L- and S-band telemetry. Proceedings of the International Telemetering Conference, Vol. IV, 1968 October. 330.

[27] Taylor, R. E.; Stocklin, R. J. VHF/UHF antenna calibration using radio stars. International Telemetering Conference Proc.; 1970 October; Vol.

VI, International Foundation for Telemetering. 375-389. Taylor, R. E. L- and S-band antenna calibration using Cass. A or Cyg. A. 1970 International Telemetry Conference; 1970 October 13-15; Vol. VI. 131-142. L-/S-band calibration error analysis. 1971 Int'l Telemetering Conference; 1971 September; Vol. VII. 528-537. Stellar calibration of L-/S-band and VHF receiving systems. NASA, 1971 July. 44.

[28] Kanda, M. An error analysis for absolute flux density measurements of Cassiopeia A. IEEE Trans. Instrum. Meas., Vol. IM-25, No. 3: 173-182; 1976 September.

[29] Kanda, M. Study of errors in absolute flux density measurements of Cassiopeia A. Nat. Bur. Stand. (U.S.) NBSIR 75-822; 1975 October. 30 p.

[30] Daywitt, W. C. An error analysis for the use of lunar radio flux in broadbeam antenna-system measurements. Submitted to IEEE Trans. Instrum. Meas.

[31] Wakefield, J. P. Earth terminal measurement system maintenance manual. Nat. Bur. Stand. (U.S.) NBSIR 78-895; 1978 September. 211 p.

[32] Wakefield, J. P. Addendum to Earth terminal measurement system maintenance manual. Nat. Bur. Stand. (U.S.) NBSIR 81-1641; 1981 October. 45 p.

[33] Daywitt, W. C. Error equations used in the NBS precision G/T measurement system. Nat. Bur. Stand. (U.S.) NBSIR 76-842; 1976 September. 17 p.

[34] Daywitt, W. C. Error equations used in the NBS Earth terminal measurement system. Nat. Bur. Stand. (U.S.) NBSIR 78-869; 1977. 25 p.

[35] Daywitt, W. C. Atmospheric propagation equations used in the NBS Earth terminal measurement system. Nat. Bur. Stand. (U.S.) NBSIR 78-883; 1978 April. 39 p.

[36] Howell, T. F.; Shakeshaft, J. R. Attenuation of radio waves by the troposphere over the frequency range 0.4-10 GHz. J. Atmospheric and Terrestrial Physics, Vol. 29, No. 7: 1559-1571; 1967 July.

[37] Yokoi, H. M.; Satoh, T. T. Atmospheric attenuation and scintillation of microwaves from outer space. Pub. Astrn. Soc. of Japan, Vol. 22, No. 4: 511; 1970.

[38] Larsen, N. T. A new self-balancing dc-substitution rf power meter. IEEE Trans. Instrum. Meas., Vol. IM-25, No. 4: 343-347; 1976 December.

[39] Ohm, E. A. Receiving system. Bell System Technical Journal, Vol. 40, No. 4: 1065-1094; 1961 July.

[40] Kanda, M. An improved solid-state noise source. IEEE Trans. Microwave Theory Techniques: 990-995; 1976 December.

[41] Boyle, D. R.; Clague, F. R.; Reeve, G. R.; Wait, D. F.; Kanda, M. An automated precision noise figure measurement system at 60 GHz. IEEE Trans. Instrum. Meas., Vol. IM-21: 543-549; 1972 November.

[42] Counas, G. J.; Bremer, T. H. NBS 30/60 megahertz noise measurement system operation and service manual. Nat. Bur. Stand. (U.S.) NBSIR 81-1656; 1981 December.

[43] Little, W. E.; Larson, W.; Kinder, B. J. Rotary-vane attenuator with an optical readout. J. of Res. Nat. Bur. Stand. (U.S.) (Eng. and Instr.). 75C(1): 1-5; 1971 January-March.

[44] Arthur, M. G.; Allred, C. M.; Cannon, M. K. A precision noise-power comparator. IEEE Trans. on Instr. and Meas., Vol. IM-13: 301-305; 1964 December.

[45] Astrophysical Quantities. The Athlone Press; 1976.

[46] Solar Geophysical Data. Edited by Helen E. Coffey, U.S. Dept. of Commerce, monthly prompt reports.

[47] Kundu, M. R. Solar Radio Astronomy. Interscience Publishers; 1965.

[48] U.S. Govt. Printing Office, Superintendent of Documents, Wash., D.C., 20402.

[49] Booker, H. G.; Gordon, W. E. A theory of radio scattering in the troposphere. Proc. I.R.E., Vol. 38: 401; 1950 April.

[50] Tatarski, V. E. Wave propagation in a turbulent medium. Dover Publications, Inc.; 1967.

NBS-114A (REV. 2-8C)

U.S. DEPT. OF COMM. BIBLIOGRAPHIC DATA SHEET (See instructions)	1. PUBLICATION OR REPORT NO. NBSIR 83-1686	2. Performing Organ. Report No.	3. Publication Date March 1983

4. TITLE AND SUBTITLE

Preliminary examination of 20 GHz G/T Measurements of Earth Terminals

5. AUTHOR(S)

D. F. Wait and W. C. Daywitt

6. PERFORMING ORGANIZATION (If joint or other than NBS, see instructions)

NATIONAL BUREAU OF STANDARDS
DEPARTMENT OF COMMERCE
WASHINGTON, D.C. 20234

7. Contract/Grant No.

8. Type of Report & Period Covered

9. SPONSORING ORGANIZATION NAME AND COMPLETE ADDRESS (Street, City, State, ZIP)

U.S. Army Communications Electronics Command
Fort Monmouth, New Jersey

10. SUPPLEMENTARY NOTES

☐ Document describes a computer program; SF-185, FIPS Software Summary, is attached.

11. ABSTRACT (A 200-word or less factual summary of most significant information. If document includes a significant bibliography or literature survey, mention it here)

Three basic measurement techniques and the associated measuring systems are examined to determine which are most likely to meet the needs of measuring the figure of merit (G/T) for future 20 GHz satellite systems: use of the Sun as a known source, use of the Sun as an intercomparison source with a calibrated reference terminal, and the use of a satellite signal as an intercomparison source. It is shown that the method of using the Sun as a known source is not very accurate (about 1.5 dB uncertainty), but that using the Sun as a transfer source is useful (0.3 dB to 0.5 dB, depending on measuring system) for Earth terminals with antenna diameter less than 1.8 m (6 ft). For Earth terminals with antenna diameters greater than 1.8 m (6 ft), the Sun cannot be used as a transfer source for technical reasons, but a satellite signal can be used as a transfer source.

12. KEY WORDS (Six to twelve entries; alphabetical order; capitalize only proper names; and separate key words by semicolons)

automated noise measurements; diffusive attenuation; figure of merit (G/T); lunar star-shape factor; millimeter wave; Moon flux; noise equivalent flux; noise measurement; satellite communications; six-port; Sun flux

13. AVAILABILITY

☒ Unlimited

☐ For Official Distribution. Do Not Release to NTIS

☐ Order From Superintendent of Documents, U.S. Government Printing Office, Washington, D.C. 20402.

☒ Order From National Technical Information Service (NTIS), Springfield, VA. 22161

14. NO. OF PRINTED PAGES 40

15. Price $8.50

☆U.S. GOVERNMENT PRINTING OFFICE:1983—678-736 / 190